Synthesis and Stability of High-Energy-Density Niobium Nitrides Under High-Pressure Conditions

Huawei Chen*, Maxim Bykov, Iskander G. Batyrev, Lukas Brüning, Elena Bykova, Mohammad F. Mahmood, Stella Chariton, Vitali B. Prakapenka, Timofey Fedotenko, Konstantin Glazyrin, Mohamed Mezouar, Gaston Garbarino, Andrew Steele, Alexander F. Goncharov

H. Chen, M. Mahmood
Department of Mathematics
Howard University, Washington DC 20059 U.S.A.
E-mail: hchen10@carnegiescience.edu

H. Chen, A. Goncharov, A. Steele

The Earth and Planets Laboratory
Carnegie Science, Washington DC, 20015, U.S.A.

M. Bykov

Institute of Inorganic and Analytical Chemistry,

Goethe University Frankfurt, Max-von-Laue-Straße 7, 60438 Frankfurt am Main, Germany

I. Batyrev

U.S. Army DEVCOM Army Research Laboratory, FCDD-RLA-WA, Aberdeen Proving Ground, Maryland, 21005 U.S.A.

L. Brüning

Institute of Inorganic and Analytical Chemistry,

Goethe University Frankfurt, Max-von-Laue-Straße 7, 60438 Frankfurt am Main, Germany

E. Bykova

Institute of Geosciences,

Goethe University Frankfurt, Altenhöferallee 1, 60438 Frankfurt am Main, Germany

S. Chariton, V, Prakapenka

Center for Advanced Radiation Sources
University of Chicago, Argonne, IL 60439, U.S.A.

T. Fedotenko, K. Glazyrin,

Deutsches Elektronene-Synchrotron DESY
Notkestr. 85, 22607 Hamburg, Germany.

M. Mezouar, G. Garbarino

European Synchrotron Radiation Facility

Grenoble Cedex F-38043 France

KEYWORDS: Polynitrides; Niobium nitrides; Energy-density; High-pressure.

ABSTRACT: High-Energy-Density materials (HEDM) are crucial in various applications, from energy storage to defense technologies. Transition metal polynitrides are promising candidates for HEDMs. Using single-crystal synchrotron X-ray diffraction, we investigated the crystal structures of niobium nitride, specifically Nb_2N_3 and NbN_2, under high-pressure conditions up to 86 GPa. At higher pressures, niobium polynitrides NbN_4 and NbN_5 were observed to be stable from 100-120 GPa that feature a low-order nitrogen bonding. The low-order bonded nitrogen in the NbN_4 and NbN_5 forms multiple polynitrogen anions at megabar pressure ranges. In the Nb-N system, we observed an increasing coordination number of metal-nitrogen as pressure increased. These structures were supported by density functional theory (DFT) calculations and Raman spectroscopy.

High pressure is known to alter the chemical composition of materials by changing the atomic arrangement within crystals, leading to the formation of high-density material. A variety of materials with unusual stoichiometries have been discovered at high pressures such as $NaCl_3$, MgO_2, FeN_4, and CoN_5.[1–4] These materials feature low-order chemical bonding, including Cl_3, O_2 ,N_4, and N_5 units. Among them, nitrides have been widely studied due to the richness of polynitrogen anions in high pressure experiments.[5–8]

Additionally, there is a growing interest in synthesizing transition metal nitrides using high-pressure apparatus such as diamond-anvil cells (DAC) and multi-anvil presses.[2,5,6,9] Studies have demonstrated the synthesis of transition metal nitrides as potential superhard materials,[10,11] high-energy-density materials,[12,13] and possible superconductors.[14] Studying the nitridation behaviors of transition metal over a wide range of pressure-temperature conditions can enhance our understanding of polynitrides under high-pressure conditions and their novel physical properties. Various new metal polynitride with nitrogen bonding order less than 3, including polynitrogen species such as N_2, N_4, N-chains and N-rings,[2,5,8,14,15] have been discovered under high-pressure conditions.

Among transition metal nitrides, niobium nitride exhibits a wide and diverse chemistry.[16,17] It is extensively studied as a superconducting material,[18,19] with ε-NbN prepared under high-pressure and high-temperature conditions demonstrating superconductivity.[19] Nb nitrides have also been investigated as potential superhard materials, including NbN[19], Nb_4N_5,[19] Nb_5N_6.[9] Higher pressure experiments have been conducted to search for Nb nitride with different nitrogen content. U_2S_3-type Nb_2N_3 was first predicted by DFT calculations[17,20] and recently synthesized in a laser-heated DAC at 30 GPa.[10] U_2S_3-type Nb_2N_3 possesses a high bulk modulus of 300 GPa.[10] Despite the importance of studying the Nb-N system and the abundance of nitrogen rich species currently discovered under high-pressure conditions,[8,12,13,21,22] research has been limited to pressures up to 31 GPa,[10] and no niobium polynitrides have been discovered in experimental studies.

Methods

We pre-indent a Re gasket and drilled a hole at the center of the indentation to form a chamber. The indented Re gasket was placed between two diamond anvils (120 um culet). We loaded niobium metal into the DAC. Pure nitrogen gas was loaded into the chamber using the gas loading system at the Earth and Planetary Laboratory of Carnegie Science. The cell was compressed to target pressures for laser heating. A piece of gold was loaded into the DAC chamber for pressure calibration.[23] The gold particles were not in contact with Nb samples to avoid chemical reactions.

Laser heating experiments were conducted at GeoSoilEnvirCars (GSECARS) at Advanced Photon Sources[24] and at the Earth and Planetary Laboratory of Carnegie Institutions for Science.[25] For a typical experiment, we steer infrared laser to the sample, and X-ray diffraction were collected during laser heating and after laser heating. We use an X-ray wavelength of 0.2952 Å at GSECARS, 0.3738 Å at ESRF, and 0.2900 Å at DESY (Deutsches Elektronen-Synchrotron).[26] Dioptas[27] software was used to integrate two-dimensional image to one dimension. X-ray diffraction patterns were collected with a duration of 1-5 seconds. Single-crystal diffraction patterns were collected after laser heating. We rotated the DAC up to 30 degrees to collect single-crystal diffractions with a step size of 0.5 degree. We used orthoenstatite crystals to calibrate the single-crystal diffraction setups. The orthoenstatite $(Mg_{1.93}Fe_{0.06})(Si_{1.93}Al_{0.06})O_6$ has a space group of *Pbca*. The lattice parameters are a = 8.812(1) Å, b = 5.183(1) Å, and c = 18.239(1) Å. We used CrysAlisPro[28] to perform data integration. DAFi (Domain Auto Finder) was adopted to search for individual grains.[29] We used Olex2[30] to solve the crystal structure using the intrinsic phasing function. We identified the atomic position for Nb and potential nitrogen positions. We refined the structure until calculated and observed single-crystal diffraction peaks matched, achieving a residue (Rwp) of less than 5%. We used GSAS-II[31] for refining the powder diffraction. Raman spectra were measured at the Earth and Planetary Laboratory of Carnegie Sciences. We measured Raman spectra on laser-heated area for 30s. A 600 groove per mm grating WiTec spectrometer was used to collect Raman spectra. We used Witec software for Raman data analysis.[32]

First-principles calculations were carried out within the framework of density functional theory (DFT)[33,34], employing the Perdew–Burke–Ernzerhof (PBE)[35] exchange-correlation functional and the plane wave/pseudopotential approach implemented in the CASTEP simulation package.[36] Norm-conserving pseudopotentials from CASTEP database were employed in conjunction with plane waves up to a kinetic energy cutoff of 770 eV. CASTEP calculates finite basis set corrections by determining the total energy at a number of cut-off energies, and then numerically evaluating the derivative required in the correction term. It is normally sufficient to use three reference points in such calculations. A Monkhorst–Pack grid was used for Brillouin zone integrations. We used a distance between grid points of <0.03 $Å^{-1}$. Convergence criteria for geometry optimization included an energy change of $<5\times10^{-8}$ eV $atom^{-1}$ between steps, a maximal force of <0.005 eV $Å^{-1}$, and a maximal component of the stress tensor <0.001 GPa. Grimme dispersion corrections were enabled.[37] Phonon frequencies were obtained from density functional perturbation theory (DFPT) calculations[38]. The phonon dispersion calculations were performed using a linear response and finite displacements method implemented in CASTEP code.[36,38]

Results and discussions

We did several experiments starting from Nb metal under nitrogen to 56-120 GPa at a temperature of 1500-1800 K. After laser heating, we observed diffraction lines that could not be indexed to Nb metal[39] and nitrogen diffraction peaks[40] (Figure S1). We solved the U_2S_3-type Nb_2N_3 at high-pressure conditions by single-crystal diffraction, the same phase was previously identified using powder diffraction at 30 GPa.[10] The unit cell parameters from single-crystal diffractions for Nb_2N_3 at 56 GPa were: a = 2.857(2) Å, b = 7.661(2) Å, and c = 7.897(1) Å in the structure with the *Pnma* space group (Table S1). There are two crystallographic sites with the same symmetry for Nb in Nb_2N_3. The Nb atoms are coordinated to 7 nitrogen atoms in Nb_2N_3 with Nb-N bonding distance range from 2.001-2.124(7) Å in the mono-capped triangular prism geometry (Figure 1). There is no N-N bonding in this structure where nitrogen should be nominally N^{3-} in Nb_2N_3. Nb has a formal oxidation state of 5+, which leave one extra electron in Nb_2N_3 ($2Nb^{5+}$, $3N^{3-}$). This extra electron should occupy the d states (half of a d band) as shown in Figure S2. The $d^{0.5}$ Nb state might be the reason for the electrical metallic conductivity in Nb_2N_3.

Table 1. Experimental runs.

Runs	Pressure (GPa)	Temperature (K)	Starting materials	Results
1	56 (4)	1700(200)	$Nb+N_2$	Nb_2N_3
2	80(4)	1500(200)	$Nb+N_2$	Nb_2N_3+NbN_2
3	86(5)	1750(200)	$Nb+N_2$	Nb_2N_3+NbN_2
4	100(4)	1800(200)	$Nb+N_2$	NbN_2+NbN_4+NbN_5
4	105(4)	1800(200)	$Nb+N_2$	NbN_4+NbN_5

Note: crystal structures are deposited in the Cambridge Crystallographic Data Center with deposition numbers CSD 2358544 (for Nb_2N_3), 2358545 (NbN_2), 2358546 (NbN_4), 2358547 (NbN_5).[41]

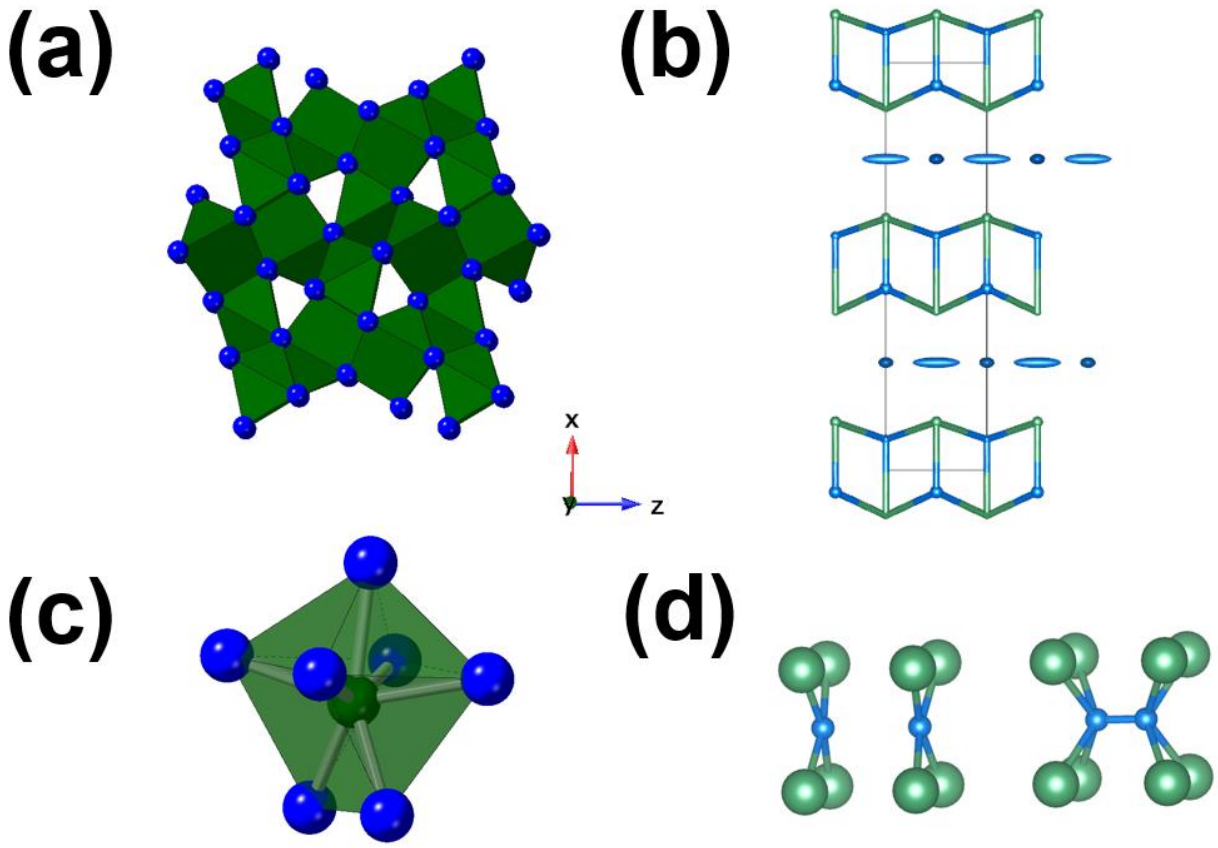

Figure 1. Crystal structures of Nb_2N_3 (a) and NbN_2 (b) from this study. In Nb_2N_3, Nb has a seven-fold coordination number with respect to nitrogen shown in (c). Crystal structure of NbN_2 refined in the space group *I*4*mm*, showing the significantly elongated thermal ellipsoids of the interlayer nitrogen atom in (b). Possible atomic coordination of N atoms in the interlayer space between Nb-N double layers (d). Green spheres indicate niobium atoms, while blue spheres indicate nitrogen atoms.

We further compressed the DAC to above 80 GPa. We heated Nb metal at this pressure, separate from the Nb_2N_3 area. After laser heating, we found strong diffraction lines that could not be indexed to any known Nb structure, nitrogen, or Nb nitrides (Figure S1).[10,39,40] Single-crystal diffraction revealed a new phase that is well-refined in the space group *I*4*mm*. The unit cell parameters are a = 2.837(1) Å, c = 11.44(1) Å. Detailed information on solving crystal structures is provided in the supplementary materials (Table S2). The structural solution and refinement in the *I*4*mm* space group reveals well-defined Nb-N double layers as shown in the Figure 1(b). Based on the difference electronic Fourier maps, the interlayer space is occupied by nitrogen atoms. The unit cell volume of the *I*4*mm* phase is consistent with the NbN_2 composition.

Locating the additional nitrogen atoms in the interlayer space presents a significant challenge due to the smaller atomic scattering factors of nitrogen compared to Nb. The refined anisotropic displacement ellipsoid of a nitrogen atom in the interlayer space shows a highly elongated shape, suggesting a split in the atomic position (Fig. 1b).

Zhao et al. [17] theoretically predicted the *oC*24-NbN_2 structure (*Cmca*) with lattice parameters a =12.496 Å, b=4.224 Å, and c=4.222 Å. This lattice is related to the experimentally determined tetragonal lattice presented here via a simple transformation $\mathbf{a_c} = \mathbf{-c_t}$, $\mathbf{b_c} = \mathbf{a_t} + \mathbf{b_t}$, $\mathbf{c_c} = \mathbf{a_c} - \mathbf{b_t}$. Refinement in this space group reveals an oscillation of nitrogen atoms between several positions in the interlayer space either forming almost square planar coordination with Nb atoms or forming dumbbells coordinated by a cube of Nb atoms (Fig. 1d). The structure refinement does not allow to choose the single model, suggesting the possibility of nitrogen atom disorder in the interlayer space. Based on the previous work [17] and our DFT calculations (Table S2), which indicate that the oC24-NbN_2 model is thermodynamically stable in the studied pressure range, we propose it as an idealized structure for NbN_2. While our experimental data generally support this model, they also point to disorder in the nitrogen layers, potentially involving the transient formation of N-N bonds (Fig. 1d). This conclusion is further supported by our calculations, which show that the square planar coordination of N atoms in NbN_2 (Table S2 and Fig. 1b) leads to imaginary frequencies in the phonon dispersion, indicating dynamic instability. However, the *Cmca* structure with dinitrogens (Figure S3) is dynamically stable. [17]

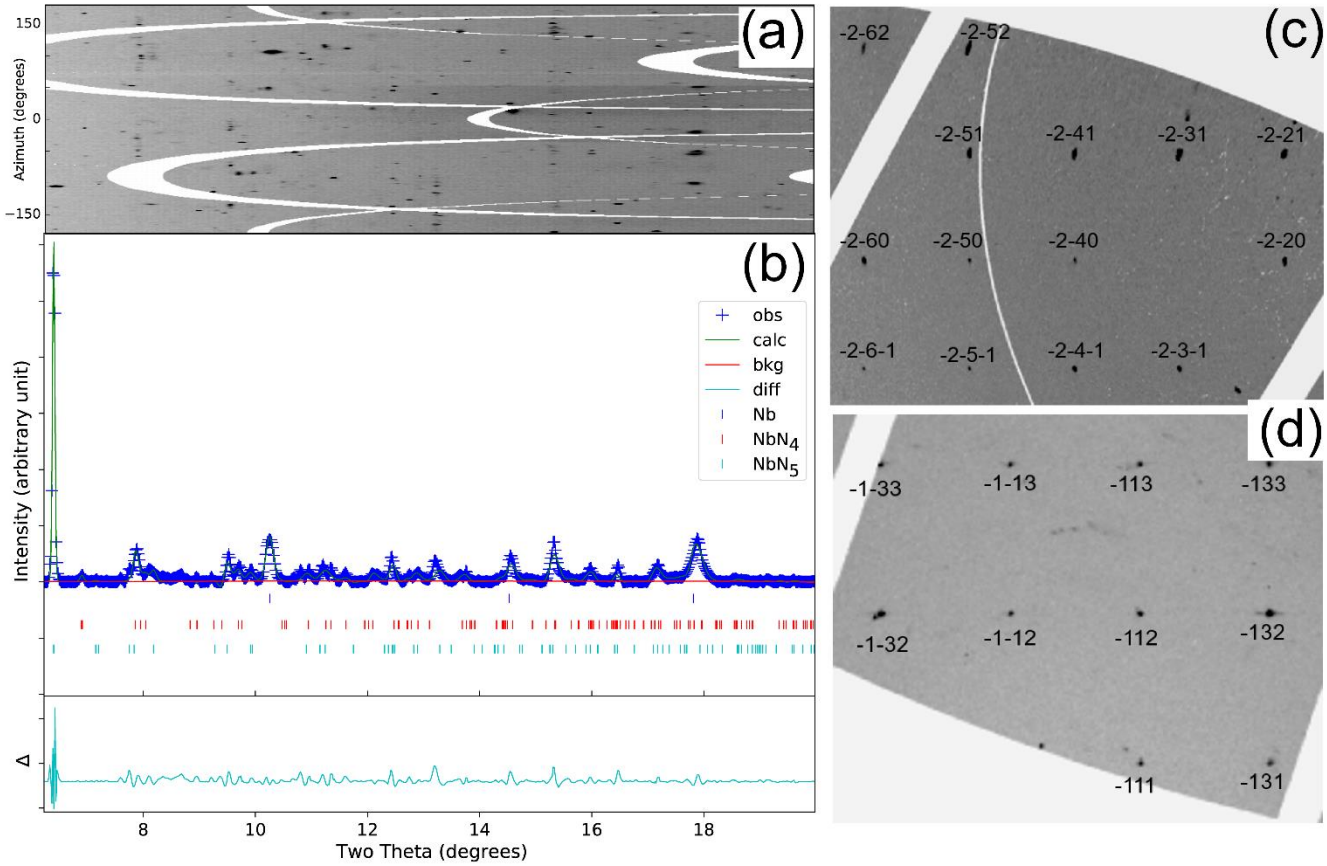

Figure 2. X-ray diffraction patterns and two-dimensional X-ray images of NbN_4 and NbN_5 ((a) and (b)). The Miller indexes are shown in the diffraction images in (c) and (d). In (c), we show reconstructed reciprocal lattice from (*-2 k l*) of NbN_4. In (d), we show diffraction images from (*-1 k l*) of NbN_5. Rietveld refinements for NbN_4 and NbN_5 (b). The residue (Rwp) for the pattern in (b) is less than 10%. The X-ray wavelength is 0.3738 Å. The ticks in (b) are the calculated positions of the diffraction lines in the NbN_4 (red) and NbN_5(blue).

Our Raman measurements did not detect any signal from the sample. This may be attributed to the metallicity of NbN_2 but could be related to disorder in the interlayer nitrogen planes. Notably, the experimentally inferred structural disorder in NbN_2 shows similarities to the incommensurate behavior reported in $TaN_{1.86}$[21] (which has similar Ta-N double layers). This behavior was explained by nonstoichiometric nitrogen composition. As in our case, dinitrogens are also not reported in $TaN_{1.86}$ and no Raman signal is detected.

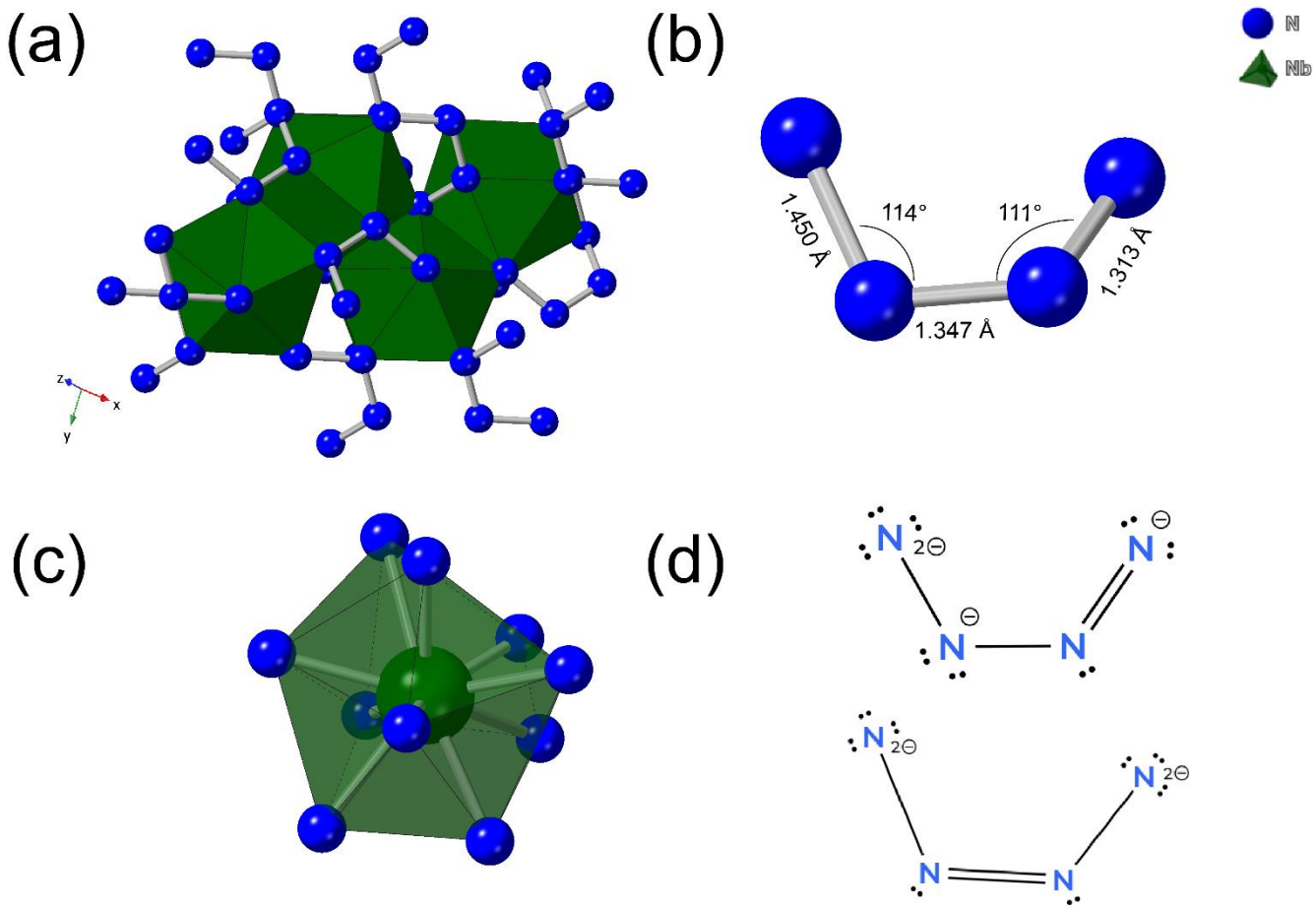

Figure 3. Crystal structure of NbN_4 under high-pressure conditions in (a). Nitrogen species in (b). 10-fold coordinated Nb with respect to nitrogen in NbN_4 is shown in (c). The Lewis structures for the nitrogen species $[N_4]^{4-}$ in (d). We provide two resonant structures for $[N_4]^4$. Uncertainties in bonding distances and angles are less than 0.005 Å and 0.1°, respectively.

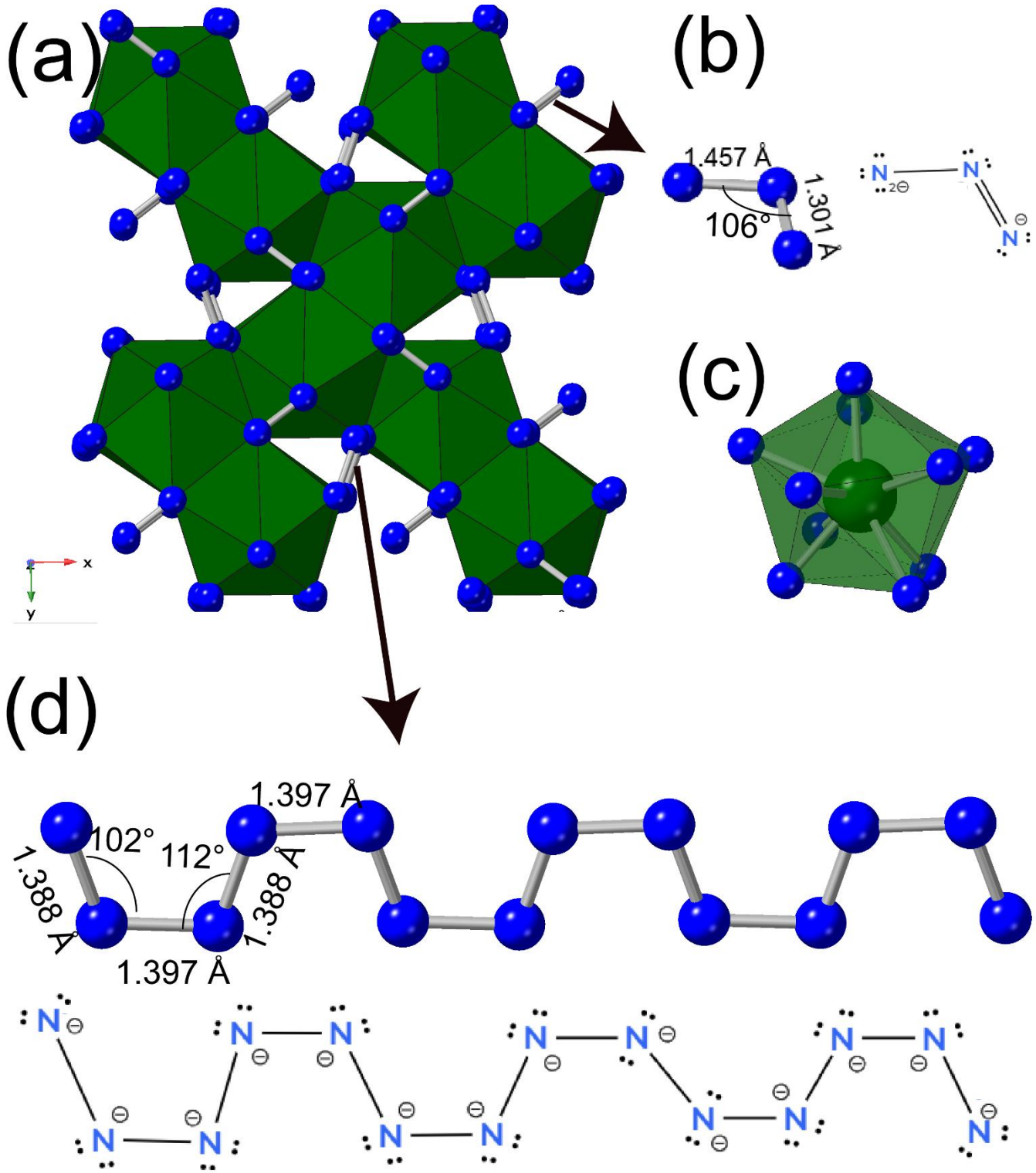

Figure 4. Crystal structure of NbN_5 under high-pressure conditions. Polynitrogen anions $[N_3]^{3-}$ and $[N_4^{4-}]_n$ in NbN_5 are shown in (b) and (d), respectively. The 10-fold coordinated Nb-N polyhedron is shown in (c). The Lewis structures for $[N_3]^{3-}$ and $[N_4^{4-}]_n$ are shown in figures. Uncertainties in bonding distance and angles are less than 0.005 Å and 0.1°, respectively.

At 100 GPa, two niobium polynitrides, NbN_4 and NbN_5, were discovered after laser heating at T>1800 K. NbN_4 crystallized in the $P2_1/n$ space group, with Nb occupying the Wyckoff 4*e* positions. The unit cell parameters are a = 4.483(1) Å, b = 5.454(1) Å, c = 5.439(9) Å, and β = 101.47(6) ° at 105 GPa (Figures 2 and 3). It is worth to note that a $P2_1/c$-NbN_4 with similar structure to our NbN_4 was predicted by DFT calculations.[17] In our NbN_4, four nitrogen atoms occupied the 4e position, resulting in the chemical formula NbN_4. Nb is coordinated to 9 nitrogen atoms with the bonding distance of Nb-N from 1.95-2.05(5) Å. One Nb-N bonding is 2.38(5) Å is much longer than other Nb-N bonding. That. The coordination number Nb to N is 10 in NbN_4. The Nb polyhedrons are of irregular shape in NbN_4. The nitrogen atoms are interconnected in the crystal structure, forming N_4 species in NbN_4 that is different the N_8 species from DFT calculations in Ref. 17. This type of N_4 polynitrogen species is also observed in TaN_4, Mg_2N_4, and Zn_2N_4 at high-pressure conditions.[6,21,22] The N-N bonding (1.31-1.45 Å) in NbN_4 is close to N-N single bonding, which gives rise to $(N_4)^{4-}$ nitrogen species. In the $(N_4)^{4-}$, three nitrogen form π bonding with bonding distance 1.31-1.35 Å, while another nitrogen is separated with a longer bonding distance (1.45 Å). The dihedral angle for the N_4 species in NbN_4 is 33(2)°, arising from repulsive long electron pair. NbN_4 has a crystal structure very similar to TaN_4

discovered at similar pressure ranges.[21] NbN_4 is found to be semi-metallic (Figure S4).

NbN_5 crystallized in the *Fdd*2 space group, where Nb is also 10-fold coordinated with N with the bonding distance of 1.93-2.29(5) Å, similar to NbN_4 (Figure 4). It is worth noting that the Nb polyhedrons are of irregular shape in NbN_5. The unit cell parameters at 105 GPa are a = 11.834(2) Å, b = 13.879(2) Å, and c = 3.600(1) Å. One Nb and five nitrogen atoms occupy the Wyckoff 16*b* positions. More complex nitrogen chemical species emerge from this structure such as nitrogen chains (N-N bonding distances=1.39-1.40 Å) and trimers. It is noteworthy that NbN_5 crystallizes in a similar crystal structure as TaN_5 in terms of space groups and atomic arrangements found in a similar pressure range. However, instead of branched-type nitrogen bonding in TaN_5, the polynitrogen ions in NbN_5 can be better described as nitrogen chains and trimers.[21] This kind of polynitride containing multiple structural units was also observed in GaN_{10} and ReN_{10}.[12,43] It is interesting to note that two lone electron pairs in a tetrahedrally coordinated nitrogen in $(N_3)^{3-}$ will lead to a N-N-N bonding angle less than 109.5°, which we observe the angle to be 106° (Figure 4b). Similar bonding angles due to the long electron pairs can be applied to the $[(N_4)^{4-}]_n$ chain in NbN_5, where a zigzag nitrogen stacking is favored over a linear chain. Theoretical calculations show that the relaxed experimental structure of NbN_5 retains all features of polynitrogens.(Figure 10 and 11) We note the bonding differences are extremely small between NbN_5 in this study and TaN_5[21]. Nevertheless, NbN_5 features a single-bonded nitrogen and NbN_5 was found to be semiconductor with a bandgap of 1.067 eV (Figure S5), where the d^0 electron configuration of Nb might contribute to the electronic structure with a band gap. It is well known that PBE method we used might underestimate the band gap.[44]

Nb_2N_3 and NbN_2 do not show any Raman spectra at pressures ranging from 56-86 GPa because of the lack of N-N bonds, which typically dominate the spectra of polynitrides. In contrast, the two polynitrides, NbN_4 and NbN_5, exhibit Raman features measured at high-pressure conditions. Distinguishing these two phases by Raman spectra is challenging due to their coexistence at high-pressure conditions. We measured a series of Raman spectra from polynitrides and N_2 areas. From the Raman spectra in Figure 5a, Raman peaks distinguishable from N_2 (Figure 5b) are clearly observed. These peaks appear to be sharp and weak, similar to Raman peaks from other polynitrides.[4,6,21,22] Notably, NbN_4 has a monoclinic structure with 30 Raman active modes ($15A_g$+$15B_g$). NbN_5 crystallizes in an orthorhombic structure, which contains 69 Raman active modes ($17A_1$+$18A_2$+$17B_1$+$17B_2$). Identifying all Raman features at high pressure conditions is challenging, especially with NbN_4 exhibiting metallic-like properties, as theoretical calculation may not calculate the Raman peak intensities in metallic systems (Figure S4).

There are three regions of the Raman spectrum that can provide structural information on polynitrides: low-frequency region (200-350 cm^{-1}), middle-frequency region (350-800 cm^{-1}), and the high-frequency region (800-1300 cm^{-1}). The low-frequency region might contain modes corresponding to translational vibrations of polynitrogen structural units in NbN_4 and NbN_5. The middle-frequency range might be related to deformation of nitrogen structural units in NbN_4 and NbN_5. The high-frequency ranges might correspond to modes closely related to N-N stretching vibrations. The calculated Raman spectra and phonon dispersions curves of NbN_5 show a good agreement with the Raman spectra from niobium polynitride at 105 GPa up to Raman wavenumbers of 1300 cm^{-1} (Figures 5 and S5).

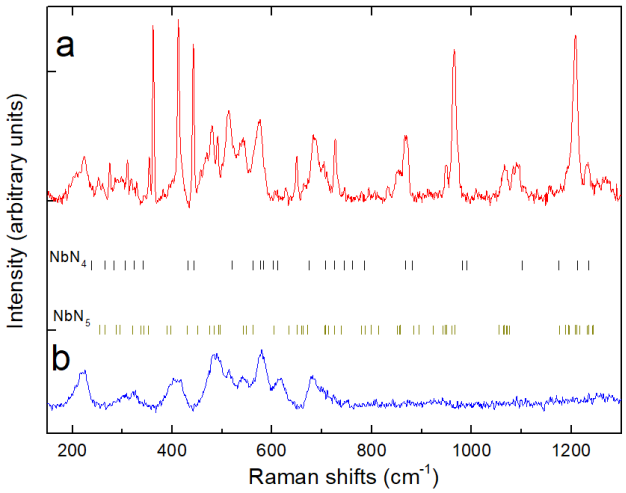

Figure 5. Raman spectra from niobium polynitrides at 105 GPa (a). (b) Raman spectra of N_2 from the same experiments. Calculated Raman peaks for NbN_4 and NbN_5 are shown in black and yellow ticks in the figure.

Our experiments on niobium nitrides show similarities with experiments on TaN_x under high-pressure conditions. Ta_2N_3, TaN_{2-x}, TaN_4, and TaN_5 were observed at high pressure conditions. The crystal structures are very similar but there are differences. NbN_2 crystallized in *I*4*mm* structure instead of the *P*4/*nmm*-structured TaN_{2-x}. Additionally, instead of branched-type nitrogen chains in TaN_5, we observed Nb being surrounded by multiple nitrogen structural units including chains and trimers. This highlights the importance of single-crystal diffraction in resolving crystal structures at high pressure conditions. Our calculated enthalpy of formation of the Nb-N system support Nb_2N_3, NbN_4 and NbN_5 as thermodynamic phases at 110 GPa (Figure S6). At 40 GPa, Nb_2N_3 and NbN_4 are stable, while NbN_5 is slightly metastable. NbN_2 is metastable at 40 and 110 GPa. Our calculations of the phonon dispersion curves show that NbN_4 and NbN_5 are dynamically stable at ambient pressure (Figures S4-S5) and 110 GPa (Figures S7-S8). We find that *Cmca* NbN_2 [17], which contains dinitrogens, is dynamically stable (Figure. S3). However, our XRD and Raman data were unable to prove the presence of dinitrogens, suggesting the stability of pernitrides in Nb nitride should be a topic of separate research.

Our experimental result generally agrees with the order of increasing Nb to N coordination number with higher pressure in Nb-N systems. We observed a 7-fold coordination number for Nb-N at 56-86 GPa in Nb_2N_3. In NbN_2, the coordination number for Nb-N changes to 9 at 86-100 GPa. In NbN_4 and NbN_5, the coordination number for Nb-N changes to 10 at 100-120 GPa. The progressive formation of nitrogen-rich species was observed at high-pressure experiments, where we only observed polynitrogen species in NbN_4 and NbN_5. It is worth noting that Fe and Co form FeN_4 and CoN_5 at megabar pressure ranges, which the crystal structures and polynitrogen anions are different from NbN_4 and NbN_5 due to the difference in the electronic structure. This emphasizes the importance of experiments on resolving the crystal structures at high pressure conditions. We note that NbN_4 and NbN_5 are not quenchable to ambient conditions from Raman measurement during decompression.

The energy density of polynitride is calculated using free the energy differences between polynitrides and nitride+N_2 phase assemblage using the equation $2NbNx=2NbN+(x-1)N_2$. Gravimetric and volumetric energy densities of NbN_4 and NbN_5 are calculated. The NbN_4 is found to have a gravimetric energy density of 1.55 kJ/g and the volumetric energy density is 11.77 kJ/cm^3. NbN_5 has a higher gravimetric energy density of 2.76 kJ/g and its volumetric energy density is 20.2 kJ/cm^3. Due to its unique mostly nitrogen single bonding, the volumetric energy density of Nb polynitrides is much higher than traditional explosives TNT (7.2 kJ/cm^3)[45] and polynitride phases such as TaN_5, ScN_5 and HfN_{10}.[13,21,45] It is worthwhile noting that the volumetric energy density of polynitrides are also related to their high density synthesized by high-pressure techniques. In sum, rational design of single-bonded nitrogen like NbN_5 might be a feasible route to achieve high energy density in polynitrides.

Overall, we identified several niobium nitrides from pressure ranging from 56-105 GPa. Two polynitrides NbN_4 and NbN_5 were found at 105 GPa. NbN_5 were found to be promising HEDM with a volumetric energy density of 20.2 kJ/cm^3. The Nb-N system shows similarities with Ta-N at high pressure conditions and the crystal structures from these two systems has differences which emphasize the importance of single-crystal diffraction techniques for structural analysis at Mbar pressures.

ASSOCIATED CONTENT

Experimental details and calculations for nitrides are in supplementary materials. This material is available free of charge via the Internet at http://pubs.acs.org.

AUTHOR INFORMATION

Corresponding Author

Huawei Chen-Department of Mathematics
Howard University, Washington DC 20059 U.S.A.
E-mail: **hchen10@carnegiescience.edu**

Authors

Maxim Bykov-Institute of Inorganic and Analytical Chemistry,

Goethe University Frankfurt, Max-von-Laue-Straße 7, 60438 Frankfurt am Main, Germany

Iskander G. Batyrev- U.S. Army DEVCOM Army Research Laboratory, FCDD-RLA-WA, Aberdeen Proving Ground, Maryland, 21005 U.S.A.

Lukas Brüning- Institute of Inorganic and Analytical Chemistry,

Goethe University Frankfurt, Max-von-Laue-Straße 7, 60438 Frankfurt am Main, Germany

Elena Bykova-Institute of Geosciences,

Goethe University Frankfurt, Altenhöferallee 1, 60438 Frankfurt am Main, Germany

Mohammad F. Mahmood-Department of Mathematics
Howard University, Washington DC 20059 U.S.A.

Stella Chariton-Center for Advanced Radiation Sources
University of Chicago, Argonne, IL 60439, U.S.A.

Vitali Prakapenka-Center for Advanced Radiation Sources
University of Chicago, Argonne, IL 60439, U.S.A.

Timofey Fedotenko -Deutsches Elektronene-Synchrotron
DESY Notkestr. 85, 22607 Hamburg, Germany.

Konstantin Glazyrin -Deutsches Elektronene-Synchrotron
DESY Notkestr. 85, 22607 Hamburg, Germany.

Andrew Steele-The Earth and Planets Laboratory
Carnegie Institution for Science. Washington DC, 20015, U.S.A.

Alexander F. Goncharov-The Earth and Planets Laboratory
Carnegie Institution for Science. Washington DC, 20015, U.S.A.

Author Contributions

The manuscript was written through contributions of all authors. All authors have given approval to the final version of the manuscript.

ACKNOWLEDGMENT

We thank the three anonymous reviewers for their insightful comments, which greatly improved the manuscript. Support is acknowledged from the National Science Foundation (NSF) DMR-2200670 and Carnegie Science. M. B. acknowledges the support of Deutsche Forschungsgemeinschaft (DFG Emmy-Noether Program project BY112/2-1). Co-funded by the European Union (ERC, HIPMAT, 101077963). Views and opinions expressed are however those of the author(s) only and do not necessarily reflect those of the EU or the ERC. Parts of this work was performed at GeoSoilEnviroCARS, Advanced Photon Source, Argonne National Laboratory. GSECARS is supported by the National Science Foundation (EAR–2223273). Advanced Photon Source is supported by Department of Energy (DOE) under Contract No. DE-AC02-06CH11357.We acknowledge the European Synchrotron Radiation Facility (ESRF) for provision of synchrotron radiation facilities under proposal numbers MA5485, CH6476, CH6817. We acknowledge DESY (Hamburg, Germany) for the provision of experimental facilities. Parts of this research were carried out at P0.2.2. Beamtime was allocated for the proposal I-20230233.

ABBREVIATIONS

Diamond-anvil Cell (DAC), High-Energy-Density Material (HEDM)

REFERENCES

(1) Zhang, W.; Oganov, A. R.; Goncharov, A. F.; Zhu, Q.; Boulfelfel, S. E.; Lyakhov, A. O.; Stavrou, E.; Somayazulu, M.; Prakapenka, V. B.; Konôpková, Z. Unexpected Stable Stoichiometries of Sodium Chlorides. *Science* **2013**, *342* (6165), 1502–1505. https://doi.org/10.1126/science.1244989.

(2) Bykov, M.; Bykova, E.; Aprilis, G.; Glazyrin, K.; Koemets, E.; Chuvashova, I.; Kupenko, I.; McCammon, C.; Mezouar, M.; Prakapenka, V.; Liermann, H.-P.; Tasnádi, F.; Ponomareva, A. V.; Abrikosov, I. A.; Dubrovinskaia, N.; Dubrovinsky, L. Fe-N System at High Pressure Reveals a Compound Featuring Polymeric Nitrogen Chains. *Nat. Commun.* **2018**, *9* (1), 2756. https://doi.org/10.1038/s41467-018-05143-2.

(3) Lobanov, S. S.; Zhu, Q.; Holtgrewe, N.; Prescher, C.; Prakapenka, V. B.; Oganov, A. R.; Goncharov, A. F. Stable Magnesium Peroxide at High Pressure. *Sci. Rep.* **2015**, *5* (1), 13582. https://doi.org/10.1038/srep13582.

(4) Chen, H.; Bykov, M.; Batyrev, I. G.; Brüning, L.; Bykova, E.; Mahmood, M. F.; Chariton, S.; Prakapenka, V. B.; Fedotenko, T.; Liermann, H.-P.; Glazyrin, K.; Steele, A.; Goncharov, A. F. High-Pressure Synthesis of Cobalt Polynitrides: Unveiling Intriguing Crystal Structures and Nitridation Behavior. *Chem. – Eur. J.* **2024**, *3*, e202400536. https://doi.org/10.1002/chem.202400536.

(5) Aslandukov, A.; Aslandukova, A.; Laniel, D.; Koemets, I.; Fedotenko, T.; Yuan, L.; Steinle-Neumann, G.; Glazyrin, K.; Hanfland, M.; Dubrovinsky, L.; Dubrovinskaia, N. High-Pressure Yttrium Nitride, Y_5N_{14}, Featuring Three Distinct Types of Nitrogen Dimers. *J. Phys. Chem. C* **2021**, *125* (32), 18077–18084. https://doi.org/10.1021/acs.jpcc.1c06210.

(6) Laniel, D.; Winkler, B.; Koemets, E.; Fedotenko, T.; Bykov, M.; Bykova, E.; Dubrovinsky, L.; Dubrovinskaia, N. Synthesis of Magnesium-Nitrogen Salts of Polynitrogen Anions. *Nat. Commun.* **2019**, *10* (1), 4515. https://doi.org/10.1038/s41467-019-12530-w.

(7) Bykov, M.; Khandarkhaeva, S.; Fedotenko, T.; Sedmak, P.; Dubrovinskaia, N.; Dubrovinsky, L. Synthesis of FeN_4 at 180 GPa and Its Crystal Structure from a Submicron-Sized Grain. *Acta Crystallogr. Sect. E Crystallogr. Commun.* **2018**, *74* (10), 1392–1395. https://doi.org/10.1107/S2056989018012161.

(8) Niwa, K.; Terabe, T.; Kato, D.; Takayama, S.; Kato, M.; Soda, K.; Hasegawa, M. Highly Coordinated Iron and Cobalt Nitrides Synthesized at High Pressures and High Temperatures. *Inorg. Chem.* **2017**, *56* (11), 6410–6418. https://doi.org/10.1021/acs.inorgchem.7b00516.

(9) Salamat, A.; Hector, A. L.; Kroll, P.; McMillan, P. F. Nitrogen-Rich Transition Metal Nitrides. *Coord. Chem. Rev.* **2013**, *257* (13), 2063–2072. https://doi.org/10.1016/j.ccr.2013.01.010.

(10) Asano, S.; Niwa, K.; Sasaki, T.; Gaida, N. A.; Hasegawa, M. Thermal Expansion of Incompressible U_2S_3-Type Nb_2N_3 Synthesized in a Diamond Anvil Cell. *Inorg. Chem.* **2020**, *59* (12), 7915–7918. https://doi.org/10.1021/acs.inorgchem.0c01057.

(11) Zerr, A.; Miehe, G.; Riedel, R. Synthesis of Cubic Zirconium and Hafnium Nitride Having Th_3P_4 Structure. *Nat. Mater.* **2003**, *2* (3), 185–189. https://doi.org/10.1038/nmat836.

(12) Bykov, M.; Bykova, E.; Koemets, E.; Fedotenko, T.; Aprilis, G.; Glazyrin, K.; Liermann, H.-P.; Ponomareva, A. V.; Tidholm, J.; Tasnádi, F.; Abrikosov, I. A.; Dubrovinskaia, N.; Dubrovinsky, L. High-Pressure Synthesis of a Nitrogen-Rich Inclusion Compound $ReN_8{\cdot}xN_2$ with Conjugated Polymeric Nitrogen Chains. *Angew. Chem. Int. Ed.* **2018**, *57* (29), 9048–9053. https://doi.org/10.1002/anie.201805152.

(13) Aslandukov, A.; Aslandukova, A.; Laniel, D.; Khandarkhaeva, S.; Yin, Y.; Akbar, F. I.; Chariton, S.; Prakapenka, V.; Bright, E. L.; Giacobbe, C.; Wright, J.; Comboni, D.; Hanfland, M.; Dubrovinskaia, N.; Dubrovinsky, L. Stabilization of N_6 and N_8 Anionic Units and 2D Polynitrogen Layers in High-Pressure Scandium Polynitrides. *Nat. Commun.* **2024**, *15* (1), 2244. https://doi.org/10.1038/s41467-024-46313-9.

(14) Liang, A.; Osmond, I.; Krach, G.; Shi, L.-T.; Brüning, L.; Ranieri, U.; Spender, J.; Tasnadi, F.; Massani, B.; Stevens, C. R.; McWilliams, R. S.; Bright, E. L.; Giordano, N.; Gallego-Parra, S.; Yin, Y.; Aslandukov, A.; Akbar, F. I.; Gregoryanz, E.; Huxley, A.; Peña-Alvarez, M.; Si, J.-G.; Schnick, W.; Bykov, M.; Trybel, F.; Laniel, D. High-Pressure Synthesis of Ultra-Incompressible, Hard and Superconducting Tungsten Nitrides. *Adv. Funct. Mater.* **2024**, *5*, 2313819. https://doi.org/10.1002/adfm.202313819.

(15) Salke, N. P.; Xia, K.; Fu, S.; Zhang, Y.; Greenberg, E.; Prakapenka, V. B.; Liu, J.; Sun, J.; Lin, J.-F. Tungsten Hexanitride with Single-Bonded Armchairlike Hexazine Structure at High Pressure. *Phys. Rev. Lett.* **2021**, *126* (6), 065702.

(16) Ivashchenko, V. I.; Turchi, P. E. A.; Olifan, E. I. Phase Stability and Mechanical Properties of Niobium Nitrides. *Phys. Rev. B* **2010**, *82* (5), 054109. https://doi.org/10.1103/PhysRevB.82.054109.

(17) Zhao, Z.; Bao, K.; Tian, F.; Duan, D.; Liu, B.; Cui, T. Phase Diagram, Mechanical Properties, and Electronic Structure of Nb–N Compounds under Pressure. *Phys. Chem. Chem. Phys.* **2015**, *17* (35), 22837–22845. https://doi.org/10.1039/C5CP02381E.

(18) Chockalingam, S. P.; Chand, M.; Jesudasan, J.; Tripathi, V.; Raychaudhuri, P. Superconducting Properties and Hall Effect of Epitaxial NbN Thin Films. *Phys. Rev. B* **2008**, *77* (21), 214503. https://doi.org/10.1103/PhysRevB.77.214503.

(19) Zou, Y.; Qi, X.; Zhang, C.; Ma, S.; Zhang, W.; Li, Y.; Chen, T.; Wang, X.; Chen, Z.; Welch, D.; others. Discovery of Superconductivity in Hard Hexagonal ε-NbN. *Sci. Rep.* **2016**, *6* (1), 1–9.

(20) Zhang, J.-D.; Huang, X.-Y. Theoretical Investigations of Structural, Electronic and Elastic Properties of U_2S_3 Type Nb_2N_3 under High Pressure. *Phys. B Condens. Matter* **2015**, *456*, 5–8. https://doi.org/10.1016/j.physb.2014.08.019.

(21) Bykov, M.; Bykova, E.; Ponomareva, A. V.; Abrikosov, I. A.; Chariton, S.; Prakapenka, V. B.; Mahmood, M. F.; Dubrovinsky, L.; Goncharov, A. F. Stabilization of Polynitrogen Anions in Tantalum–Nitrogen Compounds at High Pressure. *Angew. Chem. Int. Ed.* **2021**, *60* (16), 9003–9008. https://doi.org/10.1002/anie.202100283.

(22) Laniel, D.; Aslandukova, A. A.; Aslandukov, A. N.; Fedotenko, T.; Chariton, S.; Glazyrin, K.; Prakapenka, V. B.; Dubrovinsky, L. S.; Dubrovinskaia, N. High-Pressure Synthesis of the β-Zn_3N_2 Nitride and the α-ZnN_4 and β-ZnN_4 Polynitrogen Compounds. *Inorg. Chem.* **2021**, *60* (19), 14594–14601. https://doi.org/10.1021/acs.inorgchem.1c01532.

(23) Fei, Y.; Ricolleau, A.; Frank, M.; Mibe, K.; Shen, G.; Prakapenka, V. Toward an Internally Consistent Pressure Scale. *Proc. Natl. Acad. Sci.* **2007**, *104* (22), 9182–9186. https://doi.org/10.1073/pnas.0609013104.

(24) Prakapenka, V. B.; Kubo, A.; Kuznetsov, A.; Laskin, A.; Shkurikhin, O.; Dera, P.; Rivers, M. L.; Sutton, S. R. Advanced Flat Top Laser Heating System for High Pressure Research at GSECARS: Application to the Melting Behavior of Germanium. *High Press. Res.* **2008**, *28* (3), 225–235. https://doi.org/10.1080/08957950802050718.

(25) Goncharov, A. F.; Crowhurst, J. C. Pulsed Laser Raman Spectroscopy in the Laser-Heated Diamond Anvil Cell. *Rev. Sci. Instrum.* **2005**, *76* (6), 063905. https://doi.org/10.1063/1.1931205.

(26) Glazyrin, K.; Khandarkhaeva, S.; Fedotenko, T.; Dong, W.; Laniel, D.; Seiboth, F.; Schropp, A.; Garrevoet, J.; Brückner, D.; Falkenberg, G.; Kubec, A.; David, C.; Wendt, M.; Wenz, S.; Dubrovinsky, L.; Dubrovinskaia, N.; Liermann, H.-P. Sub-Micrometer Focusing Setup for High-Pressure Crystallography at the Extreme Conditions Beamline at PETRA III. *J. Synchrotron Radiat.* **2022**, *29* (3), 654–663. https://doi.org/10.1107/S1600577522002582.

(27) Prescher, C.; Prakapenka, V. B. DIOPTAS: A Program for Reduction of Two-Dimensional X-Ray Diffraction Data and Data Exploration. *High Press. Res.* **2015**, *35* (3), 223–230. https://doi.org/10.1080/08957959.2015.1059835.

(28) CrysAlis, P. R. O. Oxford Diffraction Ltd. *Yarnton Engl.* **2009**.

(29) Aslandukov, A.; Aslandukov, M.; Dubrovinskaia, N.; Dubrovinsky, L. Domain Auto Finder (DAFi) Program: The Analysis of Single-Crystal X-Ray Diffraction Data from Polycrystalline Samples. *J. Appl. Crystallogr.* **2022**, *55* (5), 1383–1391. https://doi.org/10.1107/S1600576722008081.

(30) Dolomanov, O. V.; Bourhis, L. J.; Gildea, R. J.; Howard, J. a. K.; Puschmann, H. OLEX2: A Complete Structure Solution, Refinement and Analysis Program. *J. Appl. Crystallogr.* **2009**, *42* (2), 339–341. https://doi.org/10.1107/S0021889808042726.

(31) Toby, B. H.; Von Dreele, R. B. GSAS-II: The Genesis of a Modern Open-Source All Purpose Crystallography Software Package. *J. Appl. Crystallogr.* **2013**, *46* (2), 544–549. https://doi.org/10.1107/S0021889813003531.

(32) Murphy, A. E.; Jakubek, R. S.; Steele, A.; Fries, M. D.; Glamoclija, M. Raman Spectroscopy Provides Insight into Carbonate Rock Fabric Based on Calcite and Dolomite Crystal Orientation. *J. Raman Spectrosc.* **2021**, *52* (6), 1155–1166. https://doi.org/10.1002/jrs.6097.

(33) Hohenberg, P.; Kohn, W. Inhomogeneous Electron Gas. *Phys Rev* **1964**, *136* (3B), B864.

(34) Kohn, W.; Sham, L. J. Self-Consistent Equations Including Exchange and Correlation Effects. *Phys Rev* **1965**, *140* (4A), A1133.

(35) Perdew, J. P.; Burke, K.; Ernzerhof, M. Generalized Gradient Approximation Made Simple. *Phys. Rev. Lett.* **1996**, *77* (18), 3865–3868. https://doi.org/10.1103/PhysRevLett.77.3865.

(36) Hafner, J. Ab-Initio Simulations of Materials Using VASP: Density-Functional Theory and Beyond. *J. Comput. Chem.* **2008**, *29* (13), 2044–2078. https://doi.org/10.1002/jcc.21057.

(37) Grimme, S. Semiempirical GGA-type density functional constructed with a long-range dispersion correction. *J. Comput. Chem.* **2006**, *27* (15), 1787–1799. https://doi.org/10.1002/jcc.20495.

(38) Segall, M. D.; Lindan, P. J. D.; Probert, M. J.; Pickard, C. J.; Hasnip, P. J.; Clark, S. J.; Payne, M. C. First-Principles Simulation: Ideas, Illustrations and the CASTEP Code. *J. Phys. Condens. Matter* **2002**, *14* (11), 2717. https://doi.org/10.1088/0953-8984/14/11/301.

(39) Kenichi, T.; Singh, A. K. High-Pressure Equation of State for Nb with a Helium-Pressure Medium: Powder X-Ray Diffraction Experiments. *Phys. Rev. B* **2006**, *73* (22), 224119. https://doi.org/10.1103/PhysRevB.73.224119.

(40) Gregoryanz, E.; Goncharov, A. F.; Hemley, R. J.; Mao, H.; Somayazulu, M.; Shen, G. Raman, Infrared, and X-Ray Evidence for New Phases of Nitrogen at High Pressures and Temperatures. *Phys. Rev. B* **2002**, *66* (22), 224108.

https://doi.org/10.1103/PhysRevB.66.224108.

(41) *Deposition numbers CSD 2358544 (for Nb_2N_3), 2358545 (NbN_2), 2358546 (NbN_4), 2358547 (NbN_5) contain the supplementary crystallographic data for this paper. These data are provided free of charge by the joint Cambridge Crystallographic Data Centre and Fachinformationszentrum Karlsruhe Access Structures service<http://www.ccdc.cam.ac.uk/structures>.*

(42) Laniel, D.; Winkler, B.; Fedotenko, T.; Aslandukova, A.; Aslandukov, A.; Vogel, S.; Meier, T.; Bykov, M.; Chariton, S.; Glazyrin, K.; Milman, V.; Prakapenka, V.; Schnick, W.; Dubrovinsky, L.; Dubrovinskaia, N. High-Pressure $Na_3(N_2)_4$, $Ca_3(N_2)_4$, $Sr_3(N_2)_4$, and $Ba(N_2)_3$ Featuring Nitrogen Dimers with Noninteger Charges and Anion-Driven Metallicity. *Phys. Rev. Mater.* **2022**, *6* (2), 023402. https://doi.org/10.1103/PhysRevMaterials.6.023402.

(43) Zhai, H.; Xu, R.; Dai, J.; Ma, X.; Yu, X.; Li, Q.; Ma, Y. Stabilized Nitrogen Framework Anions in the Ga–N System. *J. Am. Chem. Soc.* **2022**, *144* (47), 21640–21647. https://doi.org/10.1021/jacs.2c09056.

(44) Wan, Z.; Wang, Q.-D.; Liu, D.; Liang, J. Effectively Improving the Accuracy of PBE Functional in Calculating the Solid Band Gap via Machine Learning. *Comput. Mater. Sci.* **2021**, *198*, 110699. https://doi.org/10.1016/j.commatsci.2021.110699.

(45) Zhang, J.; Oganov, A. R.; Li, X.; Niu, H. Pressure-Stabilized Hafnium Nitrides and Their Properties. *Phys. Rev. B* **2017**, *95* (2), 020103. https://doi.org/10.1103/PhysRevB.95.020103.

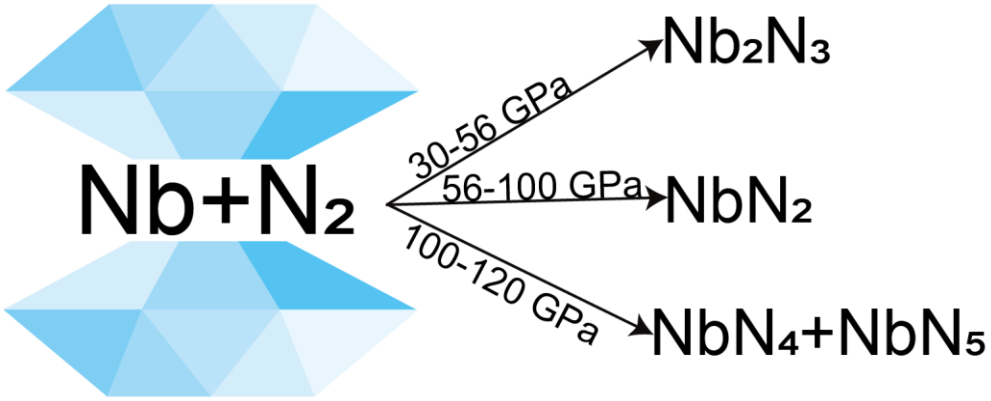

We observed a series of niobium nitrides from high pressure experiments up to 120 GPa.